Report

Current Biology

A Rapid Form of Offline Consolidation in Skill Learning

Highlights

- Temporal microscale of motor-skill learning reveals strong gains during rest periods
- Online motor-skill learning may rely largely on gains during short periods of rest
- Frontoparietal beta oscillatory activity predicts these micro-offline gains
- This rapid form of consolidation substantially contributes to early skill learning

Authors

Marlene Bönstrup, Iñaki Iturrate, Ryan Thompson, Gabriel Cruciani, Nitzan Censor, Leonardo G. Cohen

Correspondence

marlene.boenstrup@nih.gov (M.B.), cohenl@ninds.nih.gov (L.G.C.)

In Brief

Bönstrup et al. take an unprecedented close look at the time course of online motor-skill learning. They find that relevant performance improvements occur during short periods of rest. Frontoparietal beta oscillatory activity predicts those micro-offline gains. This rapid form of consolidation substantially contributes to early skill learning.

Bönstrup et al., 2019, Current Biology 29, 1346–1351
April 22, 2019 Published by Elsevier Ltd.
https://doi.org/10.1016/j.cub.2019.02.049

CellPress

CellPress

Current Biology
Report

A Rapid Form of Offline Consolidation in Skill Learning

Marlene Bönstrup,[1,4,*] Iñaki Iturrate,[2] Ryan Thompson,[1] Gabriel Cruciani,[1] Nitzan Censor,[3] and Leonardo G. Cohen[1,*]
[1]Human Cortical Physiology and Neurorehabilitation Section, National Institute of Neurological Disorders and Stroke, Bethesda, Maryland 20814, USA
[2]CNBI, Center for Neuroprosthetics (CNP), École Polytechnique Fédérale de Lausanne (EPFL), 1015 Lausanne, Switzerland
[3]School of Psychological Sciences and Sagol School of Neuroscience, Tel Aviv University, Tel Aviv 69978, Israel
[4]Lead Contact
*Correspondence: marlene.boenstrup@nih.gov (M.B.), cohenl@ninds.nih.gov (L.G.C.)
https://doi.org/10.1016/j.cub.2019.02.049

SUMMARY

The brain strengthens memories through consolidation, defined as resistance to interference (stabilization) or performance improvements between the end of a practice session and the beginning of the next (offline gains) [1]. Typically, consolidation has been measured hours or days after the completion of training [2], but the same concept may apply to periods of rest that occur interspersed in a series of practice bouts within the same session. Here, we took an unprecedented close look at the within-seconds time course of early human procedural learning over alternating short periods of practice and rest that constitute a typical online training session. We found that performance did not markedly change over short periods of practice. On the other hand, performance improvements in between practice periods, when subjects were at rest, were significant and accounted for early procedural learning. These offline improvements were more prominent in early training trials when the learning curve was steep and no performance decrements during preceding practice periods were present. At the neural level, simultaneous magnetoencephalographic recordings showed an anatomically defined signature of this phenomenon. Beta-band brain oscillatory activity in a predominantly contralateral frontoparietal network predicted rest-period performance improvements. Consistent with its role in sensorimotor engagement [3], modulation of beta activity may reflect replay of task processes during rest periods. We report a rapid form of offline consolidation that substantially contributes to early skill learning and may extend the concept of consolidation to a time scale in the order of seconds, rather than the hours or days traditionally accepted.

RESULTS

Early Online Learning Was Evidenced during Short Rest Periods

Initial training on a new motor skill consists of short periods of active practice alternating with short periods of rest, a pattern that results in significant early learning [4]. Here, we studied the relative contribution of practice and rest to early learning. 27 healthy humans practiced a well-characterized motor-skill task comprising a series of sequential key presses [5, 6], which is widely used in the study of procedural memory formation [7, 8]. They trained over 36 trials consisting of 10 s practice (reduced duration [5, 9]) and 10 s rest periods for a total of 12 min (day 1 in Figure 1A). In each practice period, participants were asked to repetitively tap a 5-item sequence indicated on the screen as quickly and accurately as possible using their left, non-dominant hand. Participants returned the following day for a test session. Performance was measured as the tapping speed (key presses/s) for correctly performed sequences [10]. We defined early learning as the window of practice trials required to reach 95% of the total day-1 learning. Modeling the group average learning curve showed that this performance level was achieved by trial 11 (Figure 1B).

During early learning, performance improved rapidly within the first few minutes of practice (Figure 1B) before reaching a performance ceiling [6, 10]. Observation of the learning curve at a high temporal within-trial resolution unveiled clear performance increments between practice periods (Figure 2A). We then proceeded to dissect learning into performance improvements occurring during the practice and rest periods. Micro-online learning was defined as the difference in tapping speed (key presses/s) between the beginning and end of each practice period. Micro-offline learning was defined as the difference in tapping speed between the end of each practice period and the beginning of the next one (Figure 2A; STAR Methods). During practice periods, performance either slightly increased, decreased, or stagnated, whereas during rest periods, we detected micro-offline gains that closely tracked total learning at a trial-by-trial basis. Micro-offline gains were maximal in early trials when performance during practice periods neither improved nor worsened (Figure 2B).

Total early learning was calculated as the sum of single-trial performance changes and amounted to 2.37 ± 0.24 key

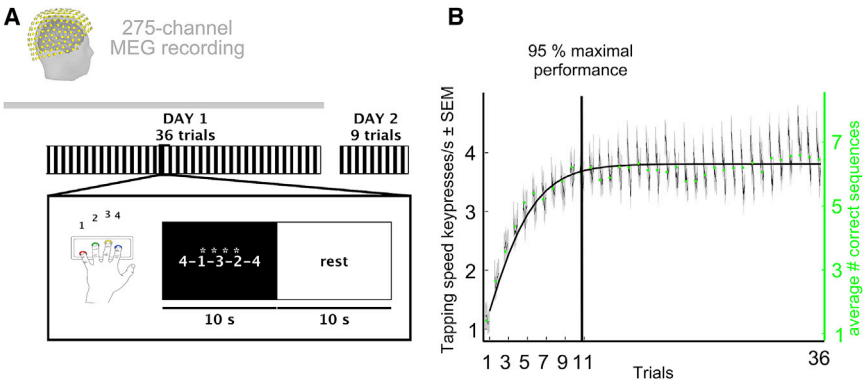

Figure 1. Motor-Skill Task and Performance Curve

(A) Task: participants learned the motor-skill task [5, 6] over 36 trials (inset shows a single trial) consisting of alternating practice and rest periods of 10 s duration for a total of 12 min. In each practice period, participants were asked to repetitively tap the sequence indicated on the screen as quickly and accurately as possible using their left, non-dominant hand. The next day, performance was tested over 9 trials. Brain oscillatory activity was recorded with magnetoencephalography (MEG) for 5 min before (resting-state baseline) and during the task on day 1.

(B) Skill was measured as the average inter-tap interval within correct sequences (tapping speed measured in key presses/s) [10]. The average number of correct sequences per trial is shown as green dots. The performance curve of day 1 (mean + SEM) and the modeled group average performance (overlaid) showed that 95% of learning occurred within the first 11 trials (vertical line, early learning) before reaching maximal performance. See also Figure S1 for supplemental behavioral data and Figure S2 for individual data.

presses/s (mean ± SEM, two-tailed one-sample t test, $T = 9.76$, $p < 0.001$). To assess the micro-online and micro-offline contribution to early learning, we summed performance differences in each participant over all 11 practice or 10 rest periods. Comparing each contribution to total early learning, we found that all early learning was accounted for by performance increases during rest periods rather than during practice periods (Figure 2C). Indeed, on average, micro-online changes were nil (−0.32 ± 0.75 key presses/s, $T = -0.41$, $p = 0.68$), whereas micro-offline gains were substantial (2.69 ± 0.63 key presses/s, $T = 4.19$, $p < 0.001$, Figures 2B and 2C).

We probed the robustness of these findings by defining micro-scale learning in alternative ways: (A) tapping speed of correct sequences in the first and last 2 s of each practice period, (B) tapping speed of correct sequences of the first and last second of each practice period, and (C) the difference in the intersection at the beginning and the end of a least-squares fit line to the performance of each practice period. All measurements rendered comparable results: early learning was evidenced during rest periods rather than during practice periods (see also Figures S1C–S1F). Performance measurements allowing within-practice-period temporal resolution of errors could conceivably provide additional information.

Learning over all day-1 trials (2.73 ± 0.22 key presses/s, mean ± SEM, two-tailed one-sample t test, $T = 12.15$, $p < 0.001$) was larger than overnight improvement from the end of training on day 1 to test on day 2 (0.73 ± 0.10 key presses/s, $T = 6.92$, $p < 0.001$), consistent with previous reports [6]. Overnight offline learning did not correlate with micro-offline gains during early learning (linear model, $p = 0.83$), suggesting different mechanisms at play. Accuracy was comparably high during early (trials 1–11; 0.89 ± 0.02, mean ± SEM) and late (trials 12–36; 0.90 ± 0.01) learning trials (Figure S1B).

Micro-Offline Learning Occurs in a State of Low Beta Power

How could learning manifest itself within 10 s rest periods? To gain insight into the systems-level possible mechanisms supporting this rapid form of offline learning, we recorded magnetoencephalographic activity during the task and in a resting-state baseline (Figure 1A). We spectrally decomposed trial-by-trial brain activity projected on the entire cortical sheet spanning rhythms that support cognitive and motor function [11]. At each location (548 edges on a cortical grid) and frequency (1–90 Hz, Figure 3A), a linear mixed effects (LME) model was estimated using oscillatory activity to predict micro-online and micro-offline learning. Micro-offline learning was inversely predicted by beta-band (16–22 Hz) brain oscillatory activity during rest periods in a predominantly contralateral frontoparietal network (Figures 3 and 4; Table S1).

This inverse relationship was confirmed by modeling micro-offline learning within participant (mean ± SEM, model coefficient, −1.23 ± 2.41, n = 27 model coefficients, $T = -2.7$, $p = 0.01$, two-tailed one-sample t test) and within trial (−0.90 ± 0.89, n = 10 model coefficients, $T = -3.2$, $p = 0.01$). The correlation between micro-offline learning and beta power during rest periods was not driven by performance improvements during early learning. First, including trial-by-trial performance in the predictive model as an additional factor (LME model with micro-offline learning as the dependent variable, beta power during rest periods and performance as fixed effects, participants as random effect, n = 10 trials × 27 participants) did not improve the model fit (likelihood ratio test, $p = 0.55$). Second, the linear partial correlation coefficient between micro-offline learning and beta power during rest periods was virtually identical with and without partialling out performance (linear partial correlation coefficient, $\rho = -0.25$, n = 10 trials × 27 participants, $p = 3.8 \times 10^{-5}$; linear correlation coefficient, $\rho = -0.26$, n = 10 trials – 27 participants, $p = 2.4 \times 10^{-5}$, respectively). Also, exclusion of the first second of the rest period (i.e., the beta rhythm amplitude rebound [12], which may include beta amplitude increase as a physiologic stop signal) from analysis (Figure S3A) did not modify this result.

In order to test whether beta rhythm amplitude predicted micro-offline gains during specific segments of the 10-s-long rest period, we estimated the same model for 5 consecutive 2-s-long segments of the rest period. The inverse prediction was stable across the entire rest period (Figure 4B). Throughout early learning, the beta rhythm power during rest periods was lower than it was during resting-state baseline (−0.1 ± 0.02, mean ± SEM, two-tailed one-sample t test, $T = -4.6$, $p = 0.001$, n = 10 trials).

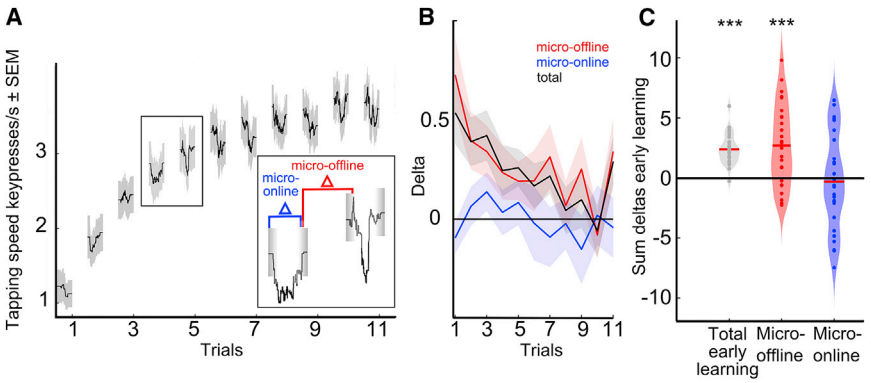

Figure 2. Early Online Learning Was Evidenced during Short Rest Periods

(A) Microscale early learning reveals performance increments over rest periods. Micro-online changes were calculated as the difference in tapping speed (key presses/s) of the first and last correct sequence within a practice period (blue in inset), and micro-offline changes were calculated as the difference between the last correct sequence within a practice period compared to the first of the next practice period (red in inset).

(B) Trial-wise early learning. Each line depicts performance changes (micro-offline in red, micro-online in blue, total in black) per trial (mean + SEM). Total learning is closely accounted for by micro-offline gains (black and red lines), whereas micro-online performance changes fluctuate around 0. Note the presence of large micro-offline gains and total early learning in the initial trials in the absence of micro-online performance decrements. Subsequently, within-practice performance decrements manifested gradually as learning slowed down.

(C) Data points in the violin plot depict the sum of changes in performance over early learning trials in each participant. Note that total early learning is accounted for by performance improvements during rest periods but not during practice periods (two-tailed one-sample t test for each learning partition, ***$p < 0.001$, FDR-corrected for multiple comparisons). See also Figure S1.

The beta rhythm emerges as transient high-powered events instead of as a sustained signal [13]. Functionally relevant differences in time-averaged power can reflect changes in event characteristics like number, amplitude, or duration. We investigated the predictive value of beta event characteristics on micro-offline learning. Beta event characteristics (number, maximum amplitude, duration) all inversely predicted micro-offline learning similarly to trial average beta power (LME, n = 10 trials × 27 participants, $p < 0.05$, Figure S4). Neither theta, alpha, or gamma rhythms during rest nor any rhythm during practice periods predicted micro-offline learning (Figures S3C and S3E). No brain oscillatory activity during practice or rest periods predicted micro-online learning (Figures S3B and S3D), learning over all day-1 trials, or overnight improvement from the end of training on day 1 to test on day 2.

DISCUSSION

The main finding of this study was that performance improvements during online procedural motor learning develop during rest instead of during practice periods. Early trials showed strongest micro-offline and total learning in the absence of preceding within-practice performance decrements. Downregulation of predominantly contralateral beta oscillatory activity during rest periods was identified as an intrinsic neural signature that predicted micro-offline gains.

Consolidation, measured as offline performance gains, has been tested at different time intervals following the end of a practice session [14, 15]. Here, we studied early performance improvements over periods of rest that occur within a series of practice bouts within the same session when naive subjects practice a new motor skill for the first time. Our results documented a substantial contribution of micro-offline performance improvements to early learning during these seconds-long rest periods in the absence of within-practice performance decrements (Figure 2B). The sum of these improvements in performance during rest periods was four times larger than it was during overnight offline learning (difference in performance between the end of training in day 1 and test on day 2), accounted for virtually all early procedural learning (Figure 2C), and represented

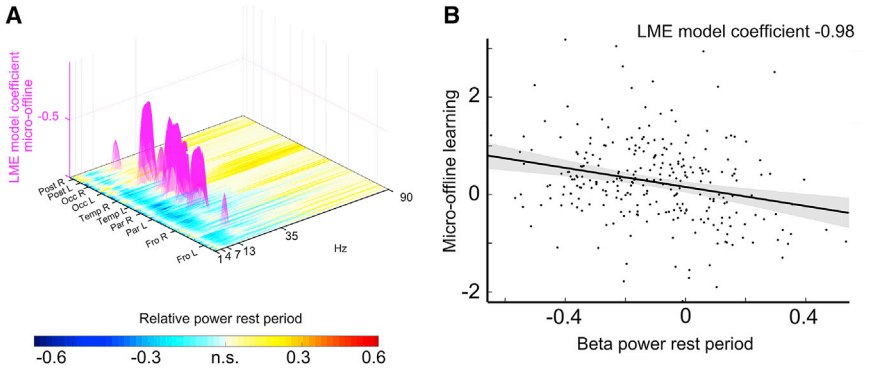

Figure 3. Micro-Offline Learning Occurs in a State of Low Beta Power

(A) Brain oscillatory activity during rest periods predictive of micro-offline learning. The horizontal plane depicts the relative power during rest periods compared to resting-state baseline across spectra (x axis, 1–90 Hz) and cortex (y axis, 548 locations clustered at frontal [Fro], parietal [Par], temporal [Temp], occipital [Occ], and cerebellar [Post] lobes). Warm yellow colors depict significant power increases during rest periods compared to resting-state baseline, cold blue colors significant power decreases (two-tailed one-sample t tests, n = 27). The z axis depicts the strength of the inverse relationship between oscillatory power and micro-offline learning (linear mixed effects (LME) model coefficient, n = 10 trials × 27 participants) at the significant frequencies and locations (magenta). All $p < 0.05$im, FDR-corrected for multiple comparisons. Note that only beta oscillatory activity at 16-22 Hz in frontoparietal areas was predictive of micro-offline learning.

(B) Inverse relationship between frontoparietal beta oscillatory activity during rest periods and micro-offline learning (n = 10 trials × 27 participants). See also Figure S3 for predictive oscillatory activity for micro-scale learning. See also Table S1.

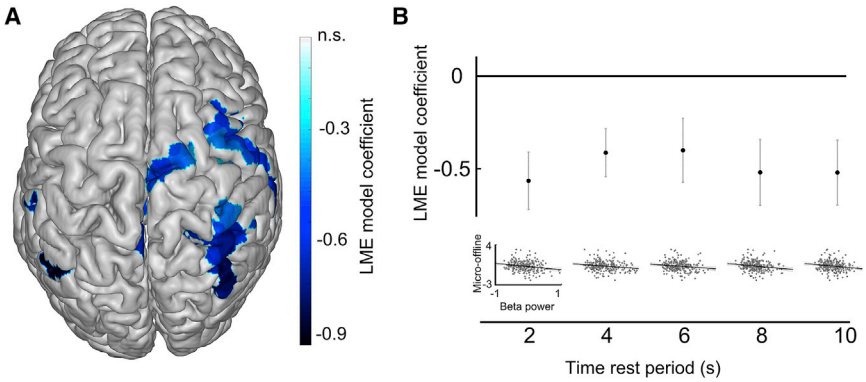

Figure 4. Topography and Time Course of Predictive Beta Oscillatory Activity for Micro-Offline Learning

(A) Topography of the predominantly contralateral beta oscillatory activity during rest periods predictive of micro-offline learning, indicated by the LME model coefficient (Table S1).

(B) Frontoparietal beta activity predicted micro-offline gains throughout the duration of early-learning rest periods (averaged in each of 5 consecutive 2 s segments, LME model coefficient ± SEM, n = 10 trials × 27 participants).

approximately 95% of overall day-1 learning for this task (Figure 1B). Thus, micro-offline gains made a sizable contribution to early motor-skill learning and to what is often referred to as initial online learning when acquiring a new motor skill [4].

The findings that micro-offline gains in this period were substantial and largest at trials with no discernible evidence of within-practice performance decrements (Figure 2B) are consistent with the interpretation that early-learning micro-offline gains may represent a rapid form of consolidation. In these early trials, micro-offline gains could conceivably result from unmasking of inhibitory effects like low-level fatigue or reactive inhibition [16]. However, previous work on rapid improvements after a few minutes of rest in the rotor pursuit task [17] have been interpreted as reflecting "the need for rest on the part of the organism in order to consolidate the memory trace" [18] rather than recovery from inhibitory effects [19]. After performance maximum was reached (i.e., following trial 11), within-practice performance decrements robustly expressed, likely signaling either fatigue or reactive inhibition (Figure S1G) [9, 20]. Optimal rest- and practice-period duration for this rapid consolidation remain to be determined.

Classically studied offline improvements in skill over extended periods of time that manifest after the end of a training session contrast with micro-offline improvements that occur early within a training session. Accordingly, we found no correlation between micro-online or micro-offline learning and overnight behavioral gains. Overnight improvements in motor skill have been linked to a topological shift of task-related neural activity from cortical to subcortical regions [10, 21] supported by a dynamic interaction between declarative (hippocampus) and procedural (striatum) memory systems [10, 22, 23]. On the other hand, the brief time window of this rapid form of consolidation points to short-term plasticity [24] rather than long-term potentiation or structural reorganization relevant for longer forms of consolidation [2].

Our finding that frontoparietal beta (16–22 Hz) oscillatory activity during rest periods predicted micro-offline learning is consistent with the involvement of the dorsal frontoparietal network in encoding offline representations of movement kinematics [16]. Recently, the beta rhythm was found to play a role in structuring short-term activity-dependent plasticity [25], qualifying it as a possible neural signature for this fast form of consolidation. A reduction of the beta rhythm amplitude is present during brain states that mediate movement preparation, execution, and imagery as well as somatosensation [3]. Thus, a low-amplitude beta rhythm reflects a state of sensorimotor engagement. It is possible that beta-related activity during rest periods may contribute to micro-offline learning through reactivation of previous practice-related activity [26, 27] or memory replay [28]. Memory replay has been documented in humans [20] during awake states [29, 30], at hippocampal [31] as well as neocortical sites [32, 33], and it may develop at a far faster rate than does the pattern of activity during memory formation [34] either in forward or reverse order [30]. This idea is consistent with observations suggesting that the reactivations involved in reconsolidation ultimately strengthen memories after an initial period of vulnerability [4, 5, 8]. GABAergic signaling, a key determinant of plasticity related to early learning [35, 36] and beta oscillations [37, 38], could possibly contribute to micro-offline gains as well. Identification of this oscillatory signature of micro-offline learning will allow future experiments to address the question of causality.

In summary, we report a rapid form of offline consolidation that contributes substantially to early skill learning. These results support the idea that the brain opportunistically consolidates previous memories whenever it is not actively learning [39], and they extend the concept of memory consolidation to a time scale on the order of seconds, rather than the hours or days traditionally accepted.

STAR★METHODS

Detailed methods are provided in the online version of this paper and include the following:

- KEY RESOURCES TABLE
- CONTACT FOR REAGENT AND RESOURCE SHARING
- EXPERIMENTAL MODEL AND SUBJECT DETAILS
  - Participants
- METHOD DETAILS
  - Task
  - Behavioral Data Analysis
  - Early learning
  - Microscale learning
  - Magnetic Resonance Imaging
  - Magnetoencephalography
  - MEG Data Analysis
  - Preprocessing
  - Source space time frequency reconstruction
  - Visualization

SUPPLEMENTAL INFORMATION

Supplemental Information can be found with this article online at https://doi.org/10.1016/j.cub.2019.02.049.

ACKNOWLEDGMENTS

We thank Kareem Zaghloul and Steven Wise for their feedback on this work. This work was supported by the German National Academy of Sciences Leopoldina (Fellowship Program grant number LPDS 2016-01 to M.B.) and by the Intramural Research Program of the National Institute of Neurological Disorders and Stroke.

AUTHOR CONTRIBUTIONS

Conceptualization, Methodology, M.B. and L.G.C.; Software, M.B. and I.I.; Validation, M.B.; Formal Analysis, M.B. and I.I.; Investigation, M.B., R.T., and G.C.; Writing, Original Draft, M.B., L.G.C., and N.C.; Review and Editing, M.B., I.I., R.T., G.C., N.C., and L.G.C.; Funding Acquisition, M.B. and L.G.C.

DECLARATION OF INTERESTS

The authors declare no competing interests.

Received: January 5, 2019
Revised: February 1, 2019
Accepted: February 21, 2019
Published: March 28, 2019

REFERENCES

1. Robertson, E.M., Pascual-Leone, A., and Miall, R.C. (2004). Current concepts in procedural consolidation. Nat. Rev. Neurosci. *5*, 576–582.
2. Squire, L.R., Genzel, L., Wixted, J.T., and Morris, R.G. (2015). Memory consolidation. Cold Spring Harb. Perspect. Biol. *7*, a021766.
3. Engel, A.K., and Fries, P. (2010). Beta-band oscillations–signalling the status quo? Curr. Opin. Neurobiol. *20*, 156–165.
4. Dayan, E., and Cohen, L.G. (2011). Neuroplasticity subserving motor skill learning. Neuron *72*, 443–454.
5. Censor, N., Horovitz, S.G., and Cohen, L.G. (2014). Interference with existing memories alters offline intrinsic functional brain connectivity. Neuron *81*, 69–76.
6. Walker, M.P., Brakefield, T., Morgan, A., Hobson, J.A., and Stickgold, R. (2002). Practice with sleep makes perfect: sleep-dependent motor skill learning. Neuron *35*, 205–211.
7. Krakauer, J.W., and Shadmehr, R. (2006). Consolidation of motor memory. Trends Neurosci. *29*, 58–64.
8. Censor, N., Sagi, D., and Cohen, L.G. (2012). Common mechanisms of human perceptual and motor learning. Nat. Rev. Neurosci. *13*, 658–664.
9. Pan, S.C., and Rickard, T.C. (2015). Sleep and motor learning: is there room for consolidation? Psychol. Bull. *141*, 812–834.
10. Vahdat, S., Fogel, S., Benali, H., and Doyon, J. (2017). Network-wide reorganization of procedural memory during NREM sleep revealed by fMRI. Elife *6*, e24987.
11. Baillet, S. (2017). Magnetoencephalography for brain electrophysiology and imaging. Nat. Neurosci. *20*, 327–339.
12. Kilavik, B.E., Zaepffel, M., Brovelli, A., MacKay, W.A., and Riehle, A. (2013). The ups and downs of β oscillations in sensorimotor cortex. Exp. Neurol. *245*, 15–26.
13. Jones, S.R. (2016). When brain rhythms aren't 'rhythmic': implication for their mechanisms and meaning. Curr. Opin. Neurobiol. *40*, 72–80.
14. Hotermans, C., Peigneux, P., Maertens de Noordhout, A., Moonen, G., and Maquet, P. (2006). Early boost and slow consolidation in motor skill learning. Learn. Mem. *13*, 580–583.
15. Doyon, J., Korman, M., Morin, A., Dostie, V., Hadj Tahar, A., Benali, H., Karni, A., Ungerleider, L.G., and Carrier, J. (2009). Contribution of night and day sleep vs. simple passage of time to the consolidation of motor sequence and visuomotor adaptation learning. Exp. Brain Res. *195*, 15–26.
16. Ptak, R., Schnider, A., and Fellrath, J. (2017). The dorsal frontoparietal network: a core system for emulated action. Trends Cogn. Sci. *21*, 589–599.
17. Eysenck, H.J. (1965). A three-factor theory of reminiscence. Br. J. Psychol. *56*, 163–182.
18. Eysenck, H.J. (1964). An experimental test of the "inhibition" and "consolidation" theories of reminiscence. Life Sci (1962) *3*, 175–188.
19. Rachman, S., and Grassi, J. (1965). Reminiscence, inhibition and consolidation. Br. J. Psychol. *56*, 157–162.
20. Rickard, T.C., Cai, D.J., Rieth, C.A., Jones, J., and Ard, M.C. (2008). Sleep does not enhance motor sequence learning. J. Exp. Psychol. Learn. Mem. Cogn. *34*, 834–842.
21. Orban, P., Peigneux, P., Lungu, O., Albouy, G., Breton, E., Laberenne, F., Benali, H., Maquet, P., and Doyon, J. (2010). The multifaceted nature of the relationship between performance and brain activity in motor sequence learning. Neuroimage *49*, 694–702.
22. Albouy, G., Fogel, S., Pottiez, H., Nguyen, V.A., Ray, L., Lungu, O., Carrier, J., Robertson, E., and Doyon, J. (2013). Daytime sleep enhances consolidation of the spatial but not motoric representation of motor sequence memory. PLoS ONE *8*, e52805.
23. Albouy, G., King, B.R., Maquet, P., and Doyon, J. (2013). Hippocampus and striatum: dynamics and interaction during acquisition and sleep-related motor sequence memory consolidation. Hippocampus *23*, 985–1004.
24. Fioravante, D., and Regehr, W.G. (2011). Short-term forms of presynaptic plasticity. Curr. Opin. Neurobiol. *21*, 269–274.
25. Zanos, S., Rembado, I., Chen, D., and Fetz, E.E. (2018). Phase-locked stimulation during cortical beta oscillations produces bidirectional synaptic plasticity in awake monkeys. Curr. Biol. *28*, 2515–2526.e4.
26. Maquet, P., Laureys, S., Peigneux, P., Fuchs, S., Petiau, C., Phillips, C., Aerts, J., Del Fiore, G., Degueldre, C., Meulemans, T., et al. (2000). Experience-dependent changes in cerebral activation during human REM sleep. Nat. Neurosci. *3*, 831–836.
27. Ramanathan, D.S., Gulati, T., and Ganguly, K. (2015). Sleep-dependent reactivation of ensembles in motor cortex promotes skill consolidation. PLoS Biol. *13*, e1002263.
28. Cohen, N., Pell, L., Edelson, M.G., Ben-Yakov, A., Pine, A., and Dudai, Y. (2015). Peri-encoding predictors of memory encoding and consolidation. Neurosci. Biobehav. Rev. *50*, 128–142.
29. Tambini, A., Ketz, N., and Davachi, L. (2010). Enhanced brain correlations during rest are related to memory for recent experiences. Neuron *65*, 280–290.
30. Foster, D.J., and Wilson, M.A. (2006). Reverse replay of behavioural sequences in hippocampal place cells during the awake state. Nature *440*, 680–683.
31. Tambini, A., and Davachi, L. (2013). Persistence of hippocampal multivoxel patterns into postencoding rest is related to memory. Proc. Natl. Acad. Sci. USA *110*, 19591–19596.
32. Yang, G., Lai, C.S., Cichon, J., Ma, L., Li, W., and Gan, W.B. (2014). Sleep promotes branch-specific formation of dendritic spines after learning. Science *344*, 1173–1178.
33. Brodt, S., Pöhlchen, D., Flanagin, V.L., Glasauer, S., Gais, S., and Schönauer, M. (2016). Rapid and independent memory formation in the parietal cortex. Proc. Natl. Acad. Sci. USA *113*, 13251–13256.

34. Euston, D.R., Tatsuno, M., and McNaughton, B.L. (2007). Fast-forward playback of recent memory sequences in prefrontal cortex during sleep. Science *318*, 1147–1150.

35. Chen, S.X., Kim, A.N., Peters, A.J., and Komiyama, T. (2015). Subtype-specific plasticity of inhibitory circuits in motor cortex during motor learning. Nat. Neurosci. *18*, 1109–1115.

36. Benali, A., Weiler, E., Benali, Y., Dinse, H.R., and Eysel, U.T. (2008). Excitation and inhibition jointly regulate cortical reorganization in adult rats. J. Neurosci. *28*, 12284–12293.

37. Yamawaki, N., Stanford, I.M., Hall, S.D., and Woodhall, G.L. (2008). Pharmacologically induced and stimulus evoked rhythmic neuronal oscillatory activity in the primary motor cortex in vitro. Neuroscience *151*, 386–395.

38. Nutt, D., Wilson, S., Lingford-Hughes, A., Myers, J., Papadopoulos, A., and Muthukumaraswamy, S. (2015). Differences between magneto-encephalographic (MEG) spectral profiles of drugs acting on GABA at synaptic and extrasynaptic sites: a study in healthy volunteers. Neuropharmacology *88*, 155–163.

39. Mednick, S.C., Cai, D.J., Shuman, T., Anagnostaras, S., and Wixted, J.T. (2011). An opportunistic theory of cellular and systems consolidation. Trends Neurosci. *34*, 504–514.

40. Oostenveld, R., Fries, P., Maris, E., and Schoffelen, J.M. (2011). FieldTrip: open source software for advanced analysis of MEG, EEG, and invasive electrophysiological data. Comput. Intell. Neurosci. *2011*, 156869.

41. Nolte, G. (2018). METH (University Medical Center Hamburg-Eppendorf). https://www.nitrc.org/projects/meth/.

42. Censor, N., Dayan, E., and Cohen, L.G. (2014). Cortico-subcortical neuronal circuitry associated with reconsolidation of human procedural memories. Cortex *58*, 281–288.

43. Censor, N., Dimyan, M.A., and Cohen, L.G. (2010). Modification of existing human motor memories is enabled by primary cortical processing during memory reactivation. Curr. Biol. *20*, 1545–1549.

44. Walker, M.P., Brakefield, T., Hobson, J.A., and Stickgold, R. (2003). Dissociable stages of human memory consolidation and reconsolidation. Nature *425*, 616–620.

45. Hardwicke, T.E., Taqi, M., and Shanks, D.R. (2016). Postretrieval new learning does not reliably induce human memory updating via reconsolidation. Proc. Natl. Acad. Sci. USA *113*, 5206–5211.

46. de Munck, J.C., van Houdt, P.J., Verdaasdonk, R.M., and Ossenblok, P.P. (2012). A semi-automatic method to determine electrode positions and labels from gel artifacts in EEG/fMRI-studies. Neuroimage *59*, 399–403.

47. Bell, A.J., and Sejnowski, T.J. (1995). An information-maximization approach to blind separation and blind deconvolution. Neural Comput. *7*, 1129–1159.

48. Tzourio-Mazoyer, N., Landeau, B., Papathanassiou, D., Crivello, F., Etard, O., Delcroix, N., Mazoyer, B., and Joliot, M. (2002). Automated anatomical labeling of activations in SPM using a macroscopic anatomical parcellation of the MNI MRI single-subject brain. Neuroimage *15*, 273–289.

49. Nolte, G. (2003). The magnetic lead field theorem in the quasi-static approximation and its use for magnetoencephalography forward calculation in realistic volume conductors. Phys. Med. Biol. *48*, 3637–3652.

50. Pascual-Marqui, R.D., Lehmann, D., Koukkou, M., Kochi, K., Anderer, P., Saletu, B., Tanaka, H., Hirata, K., John, E.R., Prichep, L., et al. (2011). Assessing interactions in the brain with exact low-resolution electromagnetic tomography. Philos Trans A Math Phys Eng Sci *369*, 3768–3784.

51. Pfurtscheller, G., and Lopes da Silva, F.H. (1999). Event-related EEG/MEG synchronization and desynchronization: basic principles. Clin. Neurophysiol. *110*, 1842–1857.

52. Shin, H., Law, R., Tsutsui, S., Moore, C.I., and Jones, S.R. (2017). The rate of transient beta frequency events predicts behavior across tasks and species. eLife *6*, e29086.

53. Benjamini, Y., and Hochberg, Y. (1995). Controlling the false discovery rate: a practical and powerful approach to multiple testing. J. R. Stat. Soc. B *57*, 289–300.

STAR★METHODS

KEY RESOURCES TABLE

REAGENT or RESOURCE	SOURCE	IDENTIFIER
Software and Algorithms		
E-prime 2	Psychology Software Tools, Inc., Sharpsburg, PA, USA	https://pstnet.com/products/e-prime/
MATLAB 2017b	The MathWorks, Natick, MA, USA	https://www.mathworks.com/products/matlab.html
FieldTrip package	[40]	http://www.fieldtriptoolbox.org/
MEG&EEG toolbox of Hamburg	[41]	https://www.nitrc.org/projects/meth/
Other		
Cedrus LS-LINE	Cedrus Corporation. San Paolo, CA, USA	https://www.cedrus.com/lumina/
GE Excite HDxt	GE Healthcare	https://www.gehealthcare.com/en/products/goldseal-refurbished-systems/goldseal-magnetic-resonance/goldseal-signa-hdxt-30t
Siemens Skyra	Siemens Healthineers, Erlangen, Germany	https://usa.healthcare.siemens.com/magnetic-resonance-imaging/3t-mri-scanner/magnetom-skyra
CTF 275 MEG system	GE Healthcare, Chicago, IL, USA	https://www.gehealthcare.com/en/products/goldseal-refurbished-systems/goldseal-magnetic-resonance/goldseal-signa-hdxt-30t

CONTACT FOR REAGENT AND RESOURCE SHARING

Further information and requests for resources should be directed to and will be fulfilled by the Lead Contact, Marlene Bönstrup (marlene.boenstrup@nih.gov).

EXPERIMENTAL MODEL AND SUBJECT DETAILS

Participants

33 naive right-handed healthy participants with a normal neurological examination gave their written informed consent to participate in the project, which was approved by the Combined Neuroscience Institutional Review Board of the National Institutes of Health (NIH). The sample size was estimated based on our prior data using the same task [5, 42]. Five participants didn't follow instructions correctly. Technical problems occurred in one recording. Full datasets were analyzed from 27 participants (17 female, mean ± SEM age 26.3 ± 0.83). Active musicians were excluded from participation [5]. Of those, 25 participants (16 female, mean ± SEM age 26.6 ± 0.87) completed the day-2 session.

METHOD DETAILS

Task

Participants learned a procedural motor-skill task on day 1 [5, 43, 44]. They used the non-dominant, left hand to perform a sequence of five key presses (4-1-3-2-4) as quickly and accurately as possible in response to instructions displayed on a monitor. Key presses were applied on a four-key response pad (Cedrus LS-LINE) with the pinky finger corresponding to button # 1, the ring finger to # 2, middle finger to # 3 and index finger to # 4 (Figure 1A). The monitor displayed the sequence continuously and provided feedback in the form of a star appearing immediately after each key press regardless of correctness. Key press timing (ms) was recorded for behavioral data analysis. 36 trials were performed during day-1 training and 9 trials were performed during day-2 testing. Each trial consisted of a 10 s practice period followed by a 10 s rest period [20, 42]. Participants were instructed to focus on the visually presented five-item sequence (during practice periods) or on five "X" symbols displayed on the monitor (during rest periods). Thus, a single trial included a practice period followed by a rest period. Each participant was tested at a similar time of day on days 1 and 2 (±2 hours). Stimuli were programmed, presented and responses recorded with E-Prime 2.

Behavioral Data Analysis

Tapping speed was quantified as the average of the time intervals between adjacent key presses within correct sequences [10] divided by 1000 (key presses/s). Performance within each trial was calculated as the mean tapping speed of all correctly performed

sequences (including correct sequences the participant has not completed by the end of the trial [44, 45]. Accuracy was quantified as 1 minus the number of erroneous relative to correct key presses in each trial [6, 45].

Early learning

The end of early learning was reached when 95% of the total day-1 learning was achieved. We chose 95% of maximal performance because it corresponds to the significance level, alpha, of 5%. It was calculated using a modeling approach in which the group average performance curve of mean tapping speed per trial, $B(t)$, was fitted using an exponential function $L(t)$:

$$B(t) \sim L(t) = k_1 + \frac{k_2}{1 + e^{-k_3 t}}$$

where k_1 and k_2 control the learning plateau, k_3 controls the learning steepness, and $t \in [1, +\infty)$ represents trial. Parameters k_{1-3} were estimated by gradient descent, with the objective function defined as the root mean square error between B and L functions:

$$\min_{\boldsymbol{k} \in \mathbb{R}^3} \sum_{t} (B(t) - L(t))^2$$

From this function, we estimated the end of early learning as the trial τ after 95% of the total learning had occurred. In practice, this value can be estimated as:

$$\tau = round\left[L^{-1}(0.95 \cdot (L(\infty) - L(1)) + L(1)) \right]$$

identifying the end of early learning at the group level by trial 11 (vertical line Figure 1B).

Microscale learning

We developed a novel approach to study trial by trial early learning, dissecting performance improvements occurring during practice (micro-online) and during rest (micro-offline) periods. Micro-online learning was defined as the difference in tapping speed between the first and the last correct sequence of a practice period. Micro-offline learning was the difference in tapping speed of the last correct sequence of a practice period and the first correct sequence of the next practice period (Figure 2A). The tapping speed of incomplete sequences was averaged with the previous complete sequence (excluding incomplete sequences from analysis elicited a comparable result, Figure S1F). In the case of only one correctly performed sequence, the speed of that sequence served as the first and last tapping speed of each trial. To derive the micro-online and micro-offline contribution to early learning we calculated the sum over all early learning trials at the participant level. The performance curve of day 1 and the modeled group average performance showed that 95% of learning occurred within the first 11 trials (Figure 1B). Thus, 11 values (practice periods) were summed for micro-online, and 10 values (rest periods) were summed for micro-offline learning. Early learning was derived as the sum of all micro-online and micro-offline values (Figure 2B). Total learning during day 1 over all 36 trials (online learning) was calculated as the difference between the mean tapping speed of the last and the first trial. Overnight improvement from the end of training on day 1 to test on day 2 was calculated as the difference between the average tapping speed of the last 9 trials of day 1 (trials 28-36) and the 9 test trials of day 2, as previously done [5, 43].

Magnetic Resonance Imaging

Structural MRI scanning was performed on a 3T MRI scanner (GE Excite HDxt and Siemens Skyra) with a standard head coil. T1-weighted high-resolution (1x1x1 mm, MPRAGE sequence) anatomical images were acquired for each participant to allow for spatial coregistration with the MEG sensors and individual head model computation.

Magnetoencephalography

MEG was recorded simultaneously with early learning during day 1, starting 5 min before the task (resting-state baseline) and for the duration of the 12 min training. MEG data were recorded using a CTF 275 MEG system composed of a whole head array of 271 (four broken sensors) radial 1st order gradiometer/SQUID channels housed in a magnetically shielded room (Vacuumschmelze, Germany) at a sampling frequency of 600 Hz. Synthetic 3rd gradient balancing was used to remove background noise online. To measure head position, three electromagnetic head coils were attached to the participant's head at the nasion, left and right pre-auricular point. The head coil positions relative to the MEG dewar were recorded at the beginning and the end of the MEG recording [46]. The task script sent synchronizing triggers via a parallel port to the MEG data acquisition computer, which were written to the MEG data file for subsequent analysis. The fiducial positions (nasion, left and right pre-auricular) of the headcoils were coregistered with the individual MRI after the MEG recording using the Brainsight Neuronavigation System (BrainSight, Rogue Research).

MEG Data Analysis

MEG data was analyzed using the FieldTrip package [40] and the MEG&EEG toolbox of Hamburg [41] on MATLAB 2017b.

Preprocessing

The continuous MEG data were band-pass filtered from 1 to 150 Hz and band-stop filtered at 60 ± 1 Hz to remove line noise using the default filter settings in the FieldTrip preprocessing functions. The artifact removal process was twofold: Fist, eyeblink, eye movement

and heart beat artifacts were removed by rejection of independent components, obtained via logisitic infomax independent component analysis [47]. Second, the entire recording was visually inspected and segments containing other artifacts like movements were visually identified and marked for rejection.

Source space time frequency reconstruction

Individual forward models consisting of 548 cortical locations and the corresponding lead field matrices were derived as follows: Based on a template anatomical brain image provided by the FieldTrip package, a regularly spaced (14 mm) three-dimensional grid of locations within the brain volume and constrained to the cortex, as defined by the AAL atlas [48], was created. This template grid was warped onto each individual MRI to give a three-dimensional grid of the same 548 cortical locations in the individual head space (source model). The choice of the spacing was a trade-off between minimizing computational load while spatially sampling the entire cortical sheet and corresponds to the reported spatial resolution of MEG [11]. Individual volume conduction models, describing how currents that are generated in the brain are propagated through the tissue to externally measurable magnetic fields, were constructed based on single-shell headmodels [49] derived from brain volume segmentation of individual MRI. Sensor positions in the MEG helmet were aligned to the individual head space by warping the MEG head coil positions (mean of pre and post recording) to the fiducials of the MRI and applying the same transformation matrix to all 271 MEG sensors. Based on the individual source and volume conduction models and the sensor positions, the lead field matrix describing the propagation of source activity from each cortical location on the grid to each MEG sensor was calculated.

Inverse solution: We reconstructed source activity using low-resolution brain electromagnetic tomography (ELORETA) which solves the inverse solution by spatial smoothness constraints [50]. For each of the 548 cortical locations two orthogonal (assuming the radial dimension is silent), real-valued spatial filters were computed that filter activity from each MEG sensor to the location of interest. The two filters were then linearly combined to a single filter in the direction of maximal variance after multiplication with the covariance matrix of the artifact free data. Using this filter, MEG time series were projected into source space to give a source space time series at each cortical location.

Spectro-temporal representations of the projected data were obtained by transforming the source space time series using Morlet wavelets at frequencies 1-90 Hz with a cycle number of 5. This procedure was done separately for the 5 min resting-state baseline and the 12 min task-related MEG recordings. To reduce inter-participant variability, each task-related time series was normalized with the corresponding average resting-state baseline power by subtraction and division following typical event-related desynchronization analysis [51]. Spectral power during practice and rest periods where averaged over the 10 s duration.

Beta event identification and characterization (Figure S4) was performed in analogy to the methodology described in [52]. Periods of high beta activity were identified in the normalized beta band (16-22 Hz) time series during rest periods by thresholding the timeseries at the 90^{th} percentile of individual average beta power. This threshold was empirically derived as the peak correlation coefficient (Pearson's) between average rest period beta power and the percent area above threshold in the non-averaged beta time series, across various thresholds (percentiles). Each suprathreshold period with a local maxima was defined as a beta event and the maximal amplitude, duration (full-width-at-half-maximum) and number of events per rest period were quantified for each participant, rest period and voxel within the cluster of predictive beta oscillatory activity for micro-offline learning (Figure 3A) and then averaged within the frontal and parietal cortex (Table S1).

Visualization

Performance curve: The within-trials time-resolved representation of tapping speed for illustration of the performance curve in Figure 1B was derived as follows: For each participant, the tapping speed at each of the 10,000 ms constituting one practice period was defined as the average inter-tap interval of the sequence the participant was executing at that moment. The duration of the execution of each sequence was defined as the time between the first key press of that sequence (or the beginning of the practice period) and the first key press of the next (or the end of the practice period). The participants' timeseries were averaged at each millisecond to give the performance curve in Figure 1B.

Topographic plots: For the topographic display of brain regions with predictive oscillatory activity (Figure 4A), the cortical grid consisting of 548 locations was interpolated onto a finer grained cortical surface of 8196 locations (provided by the FieldTrip toolbox) and spatially smoothed.

QUANTIFICATION AND STATISTICAL ANALYSIS

Behavioral data

Early learning including micro-online, micro-offline and total early learning, as well as online learning on day 1 and overnight improvement from the end of training on day 1 to test on day 2 were tested for significance using two-tailed one-sample t test. *P* values were corrected across all behavioral data statistical tests using the Benjamini & Hochberg procedure for controlling the false discovery rate (FDR) [53].

Predictive model for microscale learning

To study the relationship between early learning and brain oscillatory activity patterns we used a linear mixed-effects modeling approach. At each cortical location and oscillatory frequency, microscale learning values were modeled as the response variable

by the average spectral power as the predictor variable. Thereby, micro-online and micro-offline, as well as spectral power during practice and rest periods were modeled separately. Spectral power was modeled as a fixed effect and individual participants ID as a random effect and the fitting method used was maximum likelihood. The number of observations were 11 (micro-online) or 10 (micro-offline) trials (early learning) for each of the 27 participants (n = 297 or 270). We additionally modeled micro-offline a) within each participant, with spectral power of 10 resting periods as the predictor variable, and b) within each trial, with spectral power of 27 participants as the predictor variable. In both approaches, a linear model was used and the 27 (a) and 10 (b) model coefficients were tested for significance using two-tailed one-sample t tests. To correct for multiple comparisons across the large number of locations (548), we applied the Benjamini & Hochberg procedure [53].

DATA AND SOFTWARE AVAILABILITY

MEG and behavioral data are available upon request by contracting the Lead Contact, Marlene Bönstrup (marlene.boenstrup@nih.gov).